Arch. Mech., 42, 4–5, pp. 493–505, Warszawa 1990

Numerical studies of Rayleigh-Taylor instability by the vortex method

H. KUDELA (WROCŁAW)

THE RESULTS of a numerical investigation of Rayleigh–Taylor instability in an inviscid, incompressible flow by vortex methods was presented. The numerical procedure was briefly described. The effect of surface-tension on the smoothing of irregular motion of vortices in the vortex simulation of Rayleigh–Taylor instability is shown. The irregular motion appears as an effect of short-wave disturbances, the source of which is a round-off error. Inclusion of surface tension allows for the observation of the formation of singularities. The singularities make an infinite jump discontinuity in the curvature of the vortex sheet. It is observed that for a sufficiently small Atwood number and for initial amplitude perturbation large enough, two singularities appear in a half period of the vortex sheet and only one appears for greater Atwood numbers. The results for desingularized equations of motion were also presented. Desingularization was made by introducing the δ^2 parameter to the Cauchy type integral; in this way the singularity of the integrand was removed.

Przedstawiono wyniki badań numerycznych nad niestabilnością Rayleigha–Taylora dla cieczy nieściśliwej i nielepkiej metodą wirów punktowych. Krótko opisano algorytm numeryczny. Pokazano wygładzający wpływ napięcia powierzchniowego, które zapobiega nieregularnym ruchom wirów. Nieregularne ruchy pojawiają się jako efekt działania zaburzeń o małej długości fali, których źródłem w obliczeniach są błędy zaokrągleń. Włączenie napięcia powierzchniowego pozwala zaobserwować formowanie się osobliwości. Osobliwości te stanowią nieskończone skoki krzywizny warstwy wirowej. Zaobserwowano, że dla dostatecznie małej liczby Atwooda oraz dostatecznie dużej amplitudy zaburzenia początkowego pojawiają się dwie osobliwości w jednym półokresie warstwy wirowej, natomiast dla większej liczby Atwooda obserwuje się tylko jedną osobliwość. Przedstawiono wyniki obliczeń dla równań poddanych regularyzacji ze względu na złe uwarunkowanie zagadnienia. Regularyzacji dokonano poprzez wprowadzenie do równań ruchu parametru δ^2. Parametr ten usuwa osobliwość z funkcji podcałkowej w całkach typu Cauchy'ego.

Представлены результаты вычислительных исследований неустойчивости Рэлея–Тейлора методом точечных вихрей. Коротко описана вычислительная процедура. Показано сглаживающее действие поверхностного натяжения предупреждающее нерегулярному движению вихрей. Нерегулярное двищжение вихрей происходит за счет влияния на вычисления возмущений с короткой длиной волны, источником которых во время вычисления является ошибка округлений. Включение поверхностного натяжения позволило наблюдать создание особенностей. Эти особенности это бесконечные разрывы кривизны вихревого слоя. Наблюдалось, что для достаточно малого числа Атвуда и достаточно большой амплитуды начального возмущения возникают две особенности в одной половине периода вихревого слоя и возникает только одна особенность для большого числа Атвуда. Представлены также результаты вычислени я для регуляризованных уравнений движения. Регуляризация проведена путем введения параметра δ^2, который устраняет особенность подынтегральной функции в интеграле типа Коши.

1. Introduction

RAYLEIGH–TAYLOR (R-T) instability occurs on the interface between two fluids with different densities when the less dense fluid is accelerated in the direction of the denser one [5, 6, 22]. With some simplified assumptions, the interface can be regarded as a vortex sheet, and the investigation of its evolution can be reduced to the solution of an initial-

value problem. For the solution of this problem we can use a method based on boundary integral techniques. The velocity is expressed as an integral over some kind of singularity distributed over the fluid interface. Generally, several alternate singularity distributions can be used to represent the same interface [3, 15]. The vortex-sheet formulation described by BAKER, MEIRON, ORSZAG (B-M-O) [2] was chosen. The generalized vortex method described by B-M-O was successfully used for the case when the Atwood number $A = (\varrho_1-\varrho_2)/(\varrho_1+\varrho_2)$, $\varrho_1 > \varrho_2$ was equal to one. The method failed for $0 < A < 1$. The linear approximation of R-T, without any stabilizing mechanism, gives an arbitrarily large growth rate of short-wave length perturbations [5]. In computations, the source of short-wave perturbations is a round-off error due to finite precision arithmetics [12, 19] and without any stabilizing mechanism it leads to deterioration of calculations. Similar to Kelvin–Helmholtz instability, one may say that the problem is ill-posed in the Hadamard sense [12, 16, 20]. To suppress the chaotic, irregular motion of the vortex point, in the numerical study of vortex sheet evolution many tricks were introduced [7, 9, 12, 17]. In this paper it was demonstrated that in the R-T problem the inclusion of surface-tension effects can suppress the irregular motion of vortex points. This permits one to observe the singularity formation. The surface tension provides a small-scale stabilizing mechanism which doesn't remove the ill-posedness of the problem. To do this, a δ^2 parameter was introduced in the Cauchy-type integral to cut off the singularity of the integrand [13, 11]. The exact equations are recovered when δ^2 is set to zero. This type of regularization (desingularization) of vortex sheet evolution, also called the vortex blobs method, was first introduced by CHORIN and BERNARD [7]. Although this specific form of desingularization does not correspond precisely to a phycisal effect, it was shown by KRASNY [13] that the introduction of the δ^2 parameter acts in some sense as the viscosity. For the Kelvin–Helmholtz problem Krasny also obtained numerical evidence for the existence of the limit curve when $\delta^2 \to 0$. For the Rayleigh–Taylor problem KERR [11] found out that the limit curve probably doesn't exist but other quantities like, e.g., bubble velocity still converge. In this paper the calculations for desingularized equations were carried out only for one value of δ^2, namely $\delta^2 = 0.1$. In this situation, the surface tension caused also the lengthening of the time interval in which numerical solutions could be obtained.

2. Statement of the problem

It is assumed that the motion of the fluids is potential, two-dimensional and that the fluids are inviscid. A rectangular system of coordinates (x, y) is introduced. Before introducing a perturbation, the fluid with density ϱ_1 (ϱ_2) occupies the upper (lower) half plane and $\varrho_1 > \varrho_2$. A constant gravitational field g acts in the negative y-direction. Both ϱ_1 and ϱ_2 are constant and there is a density jump at the interface. The interface is described as a complex curve $z(a, t) = x(a, t)+iy(a, t)$ where a is regarded as a Lagrangian parameter. It is assumed that the interface and the disturbance are periodic in the x-direction with the wavelength λ_p. So $a \in [0, a_0]$ and an increment from a to a_0 gives

$$z(a+a_0, t) = z(a, t)+\lambda_p. \tag{2.1}$$

The normal velocity component on the interface is continuous (the intefrace is always

defined by the same particle) and the tangential velocity component on the interface may have a jump. So the interface can be regarded as a vortex sheet with intensity:

$$\Gamma(s, t) = (\mathbf{u}_2 - \mathbf{u}_1)\mathbf{s}^0 = \frac{\partial[\Phi]}{\partial s}, \tag{2.2}$$

where $\mathbf{u}_1, \mathbf{u}_2$ are the velocity of the upper and lower fluids at the interface, $\mathbf{s}^0$ = unit tangential vector, s — arc length, $[\Phi]$ — jump of the value of potential across the interface, t = time.

At $t = 0$, the fluid is assumed to be at rest and the flat interface $y = 0$ is perturbed and has the form $y(x, t) = \varepsilon(t)\cos Kx$ for $t > 0$. In the linear approximation [5, 19] it is known that the amplitude $\varepsilon(t)$ will behave like $\varepsilon(t) = \varepsilon(0)\mathrm{ch}\omega t$ where

$$\omega^2 = g\frac{\varrho_1 - \varrho_2}{\varrho_1 + \varrho_2}K - \frac{\sigma}{\varrho_1 + \varrho_2}K^3 \tag{2.3}$$

and where σ is the coefficient of interfacial tension, $K = 2\pi/\lambda$.

From Eq. (2.3) we see that for $\sigma = 0$, $\omega > 0$ and the interface is unstable. The growth rate for short wavelength is unbounded. Inclusion surface-tension effects ($\sigma \neq 0$) stabilize the perturbations shorter than a critical wavelength

$$\lambda_c = 2\pi\left[\frac{\sigma}{g(\varrho_1 - \varrho_2)}\right]^{1/2}. \tag{2.4}$$

To put the further equations in nondimensional form, we choose λ_p as a unit of length, $\sqrt{\lambda_p/Ag}$ as a unit of time and the surface-tensions coefficient is normalized by $g(\varrho_1 - \varrho_2)\lambda_p^2$.

3. The governing equations

By virtue of the Biot–Savart law, the induced velocity by the periodic vortex sheet at a point on the sheet can be expressed as

$$q^* = u(a, t) - iv(a, t) = \frac{1}{2i}\int_0^1 \gamma(a', t)\mathrm{ctg}\pi\big(z(a, t) - z(a', t)\big)da', \tag{3.1}$$

where $\gamma(a, t) = \Gamma(a, t)(x_a^2 + y_a^2)^{1/2}$. The subscript denotes a differentiation, and the internal is understood in the sense of the Cauchy principle value.

The vortex sheet will be replaced by suitable distribution of vortices (Lagrangian points), each of them will be labelled by parameter a. The later position of those points allow to determine the interface shape. We define the Lagrangian point velocity on the vortex sheet as follows [3, 4, 21]:

$$\frac{\partial z}{\partial t} = \frac{q_1 + q_2}{2} + \alpha\frac{q_2 - q_1}{2}, \tag{3.2}$$

where q_1, q_2 are the upper and lower limits of the fluid velocities on the interface and $\alpha \in [-1, 1]$ is a weighing factor. Note that for $\alpha = 0$ the Lagrangian point is non-material and for $\alpha = -1(1)$ it follows the upper (lower) fluid at the interface. In this way we retain some control over the positioning of the Lagrangian points. By virtue of the Sochocky–Plemelji formula [10] (see also [4]),

$$q^*_{1(2)} = q^*(\mp)\frac{\gamma}{2z_a}. \tag{3.3}$$

The velocity of a Lagrangian point on the interface can be expressed as:

$$\frac{\partial z^*}{\partial t} = q^* + \alpha \frac{\gamma}{2z_a}. \tag{3.4}$$

To Eqs. (3.3) and (3.1) the equation for vortex-sheet strength evolution due to baroclinic generation of vorticity must be added. This equation is [3]

$$\gamma_t = 2A\left(\mathrm{Re}(q_t^* z_a) - \frac{1}{2}\alpha\gamma \frac{u_a x_a + v_a y_a}{z_a z_a^*} + \frac{1}{8}\frac{\partial}{\partial a}\frac{\gamma^2}{z_a z_a^*}\right) + 2y_a - 2\sigma k_a + \frac{1}{2}\alpha \frac{\partial}{\partial_a}\frac{\gamma^2}{z_a z_a^*}, \tag{3.5}$$

where $k = (x_a y_{aa} - y_a x_{aa})/(x_a^2 + y_a^2)^{1,5}$ — the curvature of the vortex sheet, σ = the non-dimensional coefficient of surface tension. The time derivatives q_t^* are obtained by differentiation of Eq. (3.1). After substitution of these derivatives to (3.5), we can obtain

$$\gamma_t = A \int_0^1 \gamma_t B da' + r(x, y, u, v, \gamma), \tag{3.6}$$

(the integral is understood in the sense of the Cauchy principal value), where

$$B = -x_a \frac{\mathrm{sh}\,2\pi(y(a) - y(a'))}{\mathrm{ch}\,2\pi(y(a) - y(a')) - \cos 2\pi(x(a) - x(a'))} + y_a \frac{\sin 2\pi(x(a) - x(a'))}{\mathrm{ch}\,2\pi(y(a) - y(a')) - \cos 2\pi(x(a) - x(a'))}$$

and $r(\ )$ does not depend on γ_t. Equation (3.6) represents by itself the Fredholm integral equation of the second kind and is solved iteratively. As has already been mentioned in the introduction, the initial value problem for R-T is ill-posed. The solution within a finite time yields the singularity which is an infinite jump in the curvature. In order to regularize the problem, the singularity of the integrand of the Cauchy-type integral is cut off. The components of velocity of Eq. (5) are now

$$u(a, t) = -\frac{1}{2}\int_0^1 \frac{\gamma(a', t)\,\mathrm{sh}\,2\pi(y(a) - y(a'))}{\mathrm{ch}\,2\pi(y(a) - y(a')) - \cos 2\pi(x(a) - x(a') + \delta^2}\, da',$$

$$v(a, t) = \frac{1}{2}\int_0^1 \frac{\gamma(a', t)\sin 2\pi(x(a) - x(a'))}{\mathrm{ch}\,2\pi(y(a) - y(a')) - \cos 2\pi(x(a) - x(a')) + \delta^2}\, da'. \tag{3.1'}$$

Now the integrals in Eqs. (3.1') are not singular and if we calculate with the assistance of Eqs. (3.1') the acceleration u_t, v_t, Eq. (3.6) also will not have a singular integral. In the case of weak stratification when $\varrho_1/\varrho_2 \to 1$, the Boussinesq asymptotic approximation is often made. We take $A \to 0$ and $g \to \infty$ in such a way that the product Ag goes to the finite limit [20]. Equation (3.5) takes the form ($\alpha = 0$):

$$\gamma_t = 2y_a - 2\sigma k_a. \tag{3.5'}$$

Equations (3.4) and (3.6) constitute the complete description of the evolution for the interface. The numerical procedure goes as follows [3]: for known $x(a)$, $y(a)$, $\gamma(a)$ the inter-

face is marched forward using Eqs. (3.4) and (3.1) and next the inhomogeneous term $r(\ )$ in Eq. (3.6) is calculated. Then the integral equation (3.6) is solved iteratively for γ and finally γ can be also marched in time. When we use the Boussinesq approximation, we do not need to solve the integral equation and γ_t is simply calculated from Eq. (3.5'). The time stepping is performed by using the fourth-order Adam–Moulton predictor-corrector scheme. All derivatives with respect to the Lagrangian parameter a were computed using cubic splines. All Cauchy type integrals were regularized by subtraction of the integral with a known principal value [3] and integrals were calculated using the trapezoid rule on alternate sets of points [4].

4. Numerical results

The results presented below were obtained on an IBM PC-AT in double precision (15 decimal digits) arithmetics using RMFORTRAN. The number of vortices accepted for calculations is $N = 120$, time step $\Delta t = 0.004$. Figures 1a, b, c, d show solutions for $A = 1$ ($\varrho_1/\varrho_2 =$ so-called single fluid case). Figure 1a shows a time sequence of interface profile $y(x, t)$, Fig. 1b shows time sequence of vortex sheet strength $\Gamma(a, t)$ vs Lagrangian parameter a, Fig. 1c the velocity vs time at the peak of the bubble ($x = 0$) and Fig. 1d accelera-

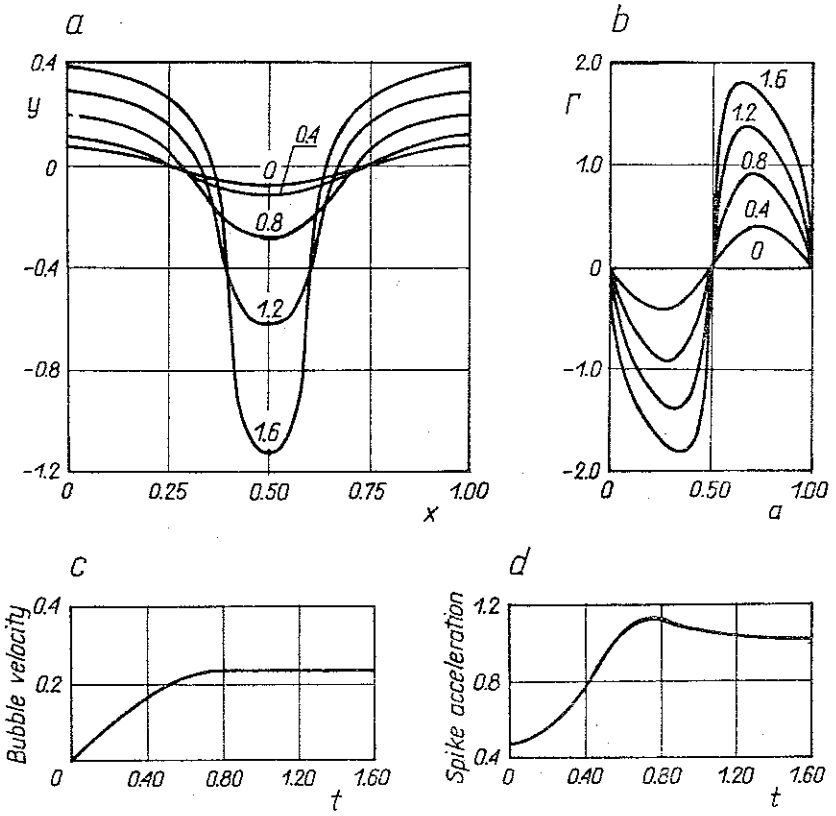

FIG. 1. Numerical results for the Atwood ratio $A = 1$, $\alpha = -1$, $\delta^2 = 0$, $\sigma = 0$; a) sequence of interface profile $y(x, t)$, b) sequence of vortex sheet strength Γ vs Lagrangian parameter a, c) a plot of the velocity vs time at the peak ($x = 0$) of the bubble, d) a plot of acceleration vs time at the tip ($x = 0.5$) of the spike.

tion vs time at the tip of the spike ($x = 0.5$), $y(x, 0) = \varepsilon \cos 2\pi x$, $\varepsilon = 0.5/2\pi$ was taken as the initial condition. Such an amplitude makes it possible to compare results with [2] (see also [18]). These single fluid case results were described precisely by B-M-O [2] and can be regarded as an "exact" solution. It is a good test for the program. For α in Eq. (3.2) $\alpha = -1$ was accepted. This means that vortices move like the particles of the upper fluid.

Figures 2a, b, c show numerical results for $A = 0.0476$ ($\varrho_1/\varrho_2 = 1.1$) $\varepsilon = 0.1$, $\delta^2 = 0$ (exact equations), $\sigma = 0$ (without surface tension). Figure 2a shows the time sequence of interface profiles (only half a period) and Fig. 2b the time sequence of the curvature $k(a)$ of the interface and Fig. 2c shows the time sequence of vortex sheet strength $\Gamma(a)$. The inspection of curvature is a good means of checking the smoothness of the solutions and it shows the symptoms of the regularity loss of the solution earlier than one can see on interface profile. In Fig. 2b for $t = 0.74$ one can see the irregular, noisy changes of curvature at the interval where vortex sheet strength has its maximum approximately. It is due to Helmholtz instability. Those noisy changes start a little earlier and their amplitude grows in time.

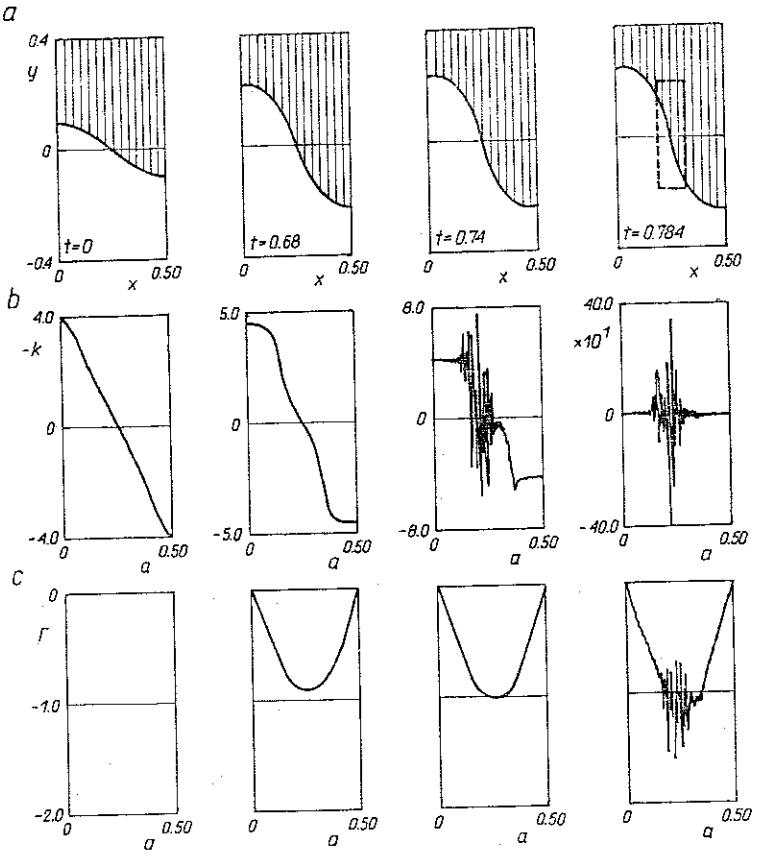

FIG. 2. Numerical results for $A = 0.0476$ ($\varrho_1/\varrho_2 = 1.1$), $\alpha = 0$, $\delta^2 = 0$, $\sigma = 0$ (without surface tension), $y(x, 0) = 0.1\cos 2\pi x$, $\gamma(x, 0) = 0$; a) time sequence of interface profile $y(x, t)$, b) sequence of curvature $-k$ vs Lagrangian parameter a, c) sequence of vortex sheet strength Γ vs Lagrangian parameter a. Values of t as shown in Fig. 2a .

Figure 3 shows the time sequence of the close-up fragments of the interface matched by the frame in Fig. 2a $t = 0.784$. These fragments are defined by the same particles. For $t = 0.784$ the irregular position of vortices is seen distinctly.

Figures 4a, b show the time sequence of the curvature and strength of the vortex sheet in the case when the surface-tension effects were included. We took $\sigma = 5 \times 10^{-4}$. Now the noisy, chaotic changes don't appear in the curvature. The curvature distribution for $t = 0.824$ has two peaks and typical tips appear in the distribution of vortex strength.

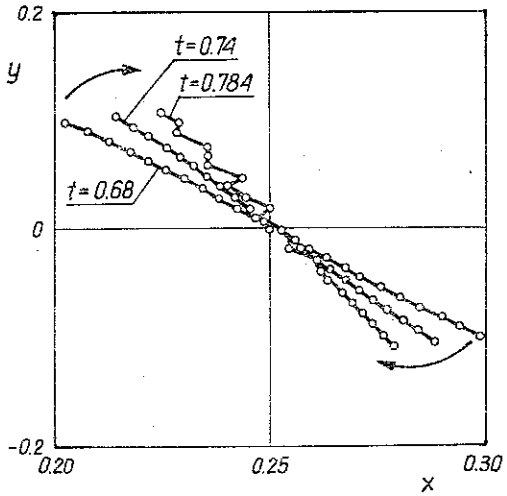

FIG. 3. Close-up fragments of interface profile which are created by the same particles for the data as in Fig. 2. Values of t as shown.

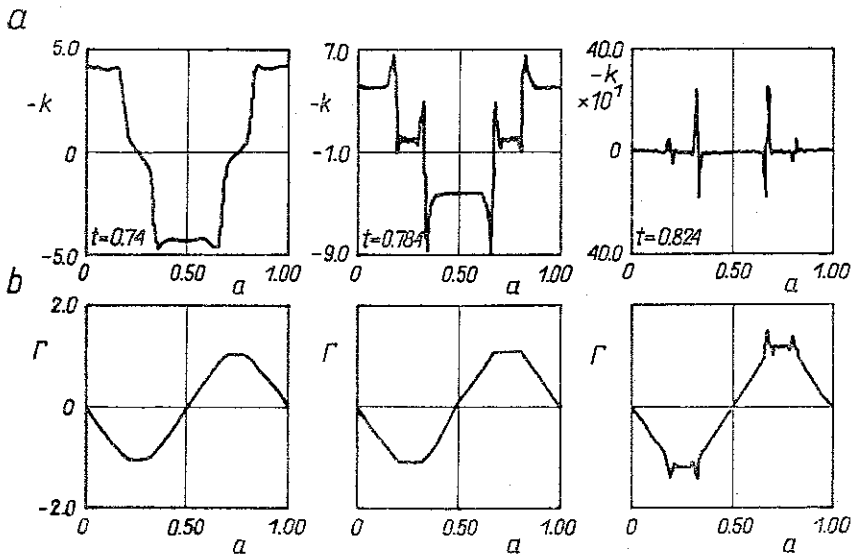

FIG. 4. Numerical results for the data as in Fig. 2 but this time with surface tension $\sigma = 0.0005$; a) sequence of curvature $-k$ vs Lagrangian parameter a, b) time sequence of vortex sheet strength Γ vs Lagrangian parameter a. Values of t as shown in Fig. 4a.

Figure 5 shows the time sequence of the close-up fragments of the interface defined by the same particle as in Fig. 3. The origination of cusps is visible and it can be related to formation of singularities. The suppression of the irregular motion of vortices is evident. The formation of two singular points is connected with the large initial amplitude of perturbation ($\varepsilon = 0.1$). For $\varepsilon = 0.01$ we can observe only one singularity along half a period of the interface.

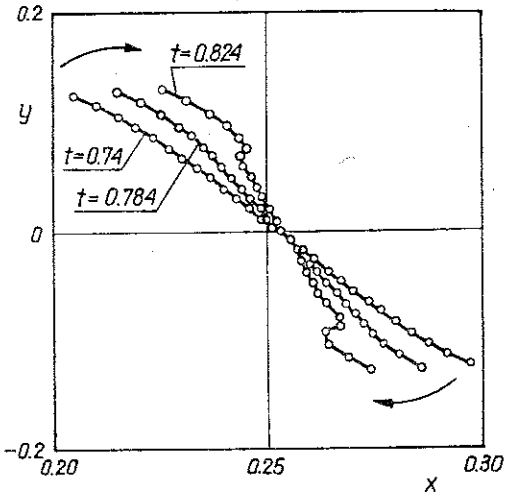

FIG. 5. Sequence of close-up interface fragments from Fig. 4a which are created by the same particles (Lagrangian points) for included surface-tension effects $\sigma = 0.0005$.

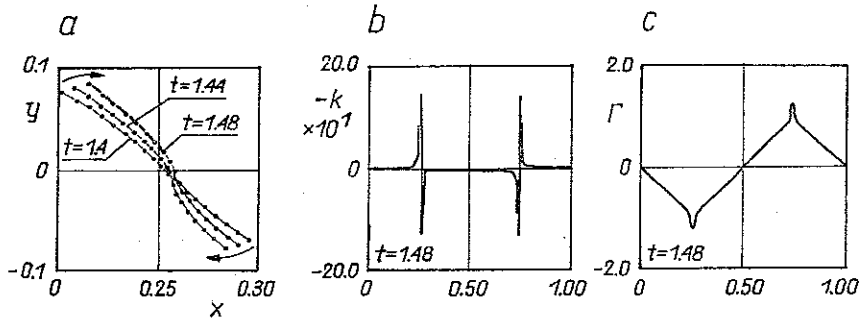

FIG. 6. Numerical results for data as in Fig. 4 but with initial amplitude $\varepsilon = 0.01$, a) time sequence of the close-up fragments of interface, b) curvature k vs Lagrangian parameter a for $t = 1.48$, c) vortex sheet strength Γ vs parameter a for $t = 1.48$.

Figure 6a shows the time sequence of close-up fragments of the interface and Figs. 6b, c show examples of the curvature distribution and vortex sheet strength for time $t = 1.48$. The results which relate to the singularity formation, which I present here, are very similar to the results presented by KRASNY [9]. For a larger Atwood number, in spite of $\varepsilon = 0.1$, only one singularity originates.

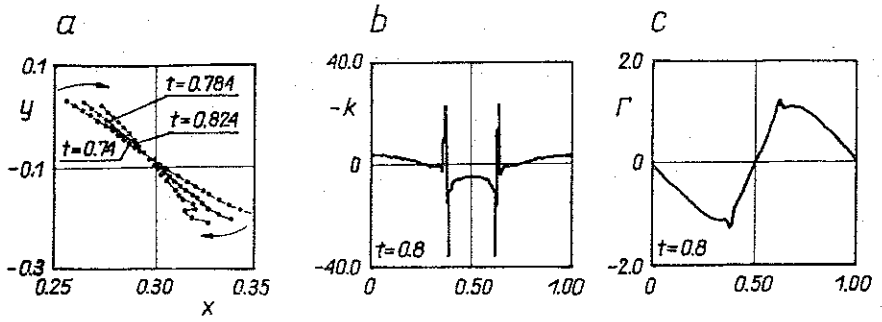

FIG. 7. Numerical results for $A = 0.5$ ($\varrho_1/\varrho_2 = 3$), $\sigma = 0.0005$, $\alpha = -0.2$, $\varepsilon = 0.1$; a) sequence of close-up fragments of interface. Values of t as shown, b) curvature of interface $-k$ vs parameter a for $t = 0.8$ c) vortex sheet strength vs parameter a $\Gamma(a)$ for $t = 0.8$.

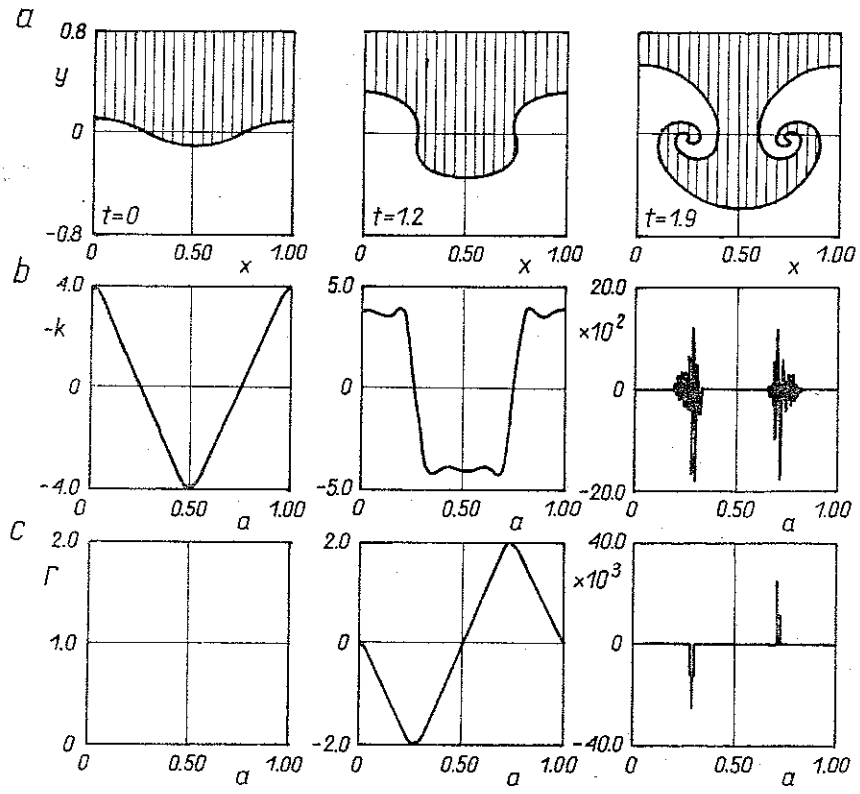

FIG. 8. Numerical results for desingularized equation, $\delta^2 = 0.1$, $A = 0.0476$ ($\varrho_1/\varrho_2 = 1.1$), $\sigma = 0.0005$, $\alpha = 0$ and initial condition as in Fig. 2; a) time sequence of interface profiles $y(x, t)$, b) sequence of curvature $-k$ vs Lagrangian parameter a, c) sequence of vortex sheet strength Γ vs parameter a. Values of t as shown in Fig. 8a.

Figure 7 show results for $A = 0.5$. Figure 7a shows the time sequence of close-up of interface fragments and Fig. 7b, c the example of curvature and vortex sheet strength $\Gamma(a)$ distribution for $t = 0.8$. The singularity formation in solutions is the reason why the B-M-O method failed for $0 < A < 1$. In order to regularize the initial value problem for the vortex sheet in constant density, KRASNY [13, 14] proposed to introduce to the equation of motion the δ^2 parameter (Eq. 3.1'). But in the case of the R-T problem, regularization by introducing δ^2 is not so efficient as it was demonstrated by Krasny. Due to the nonlinearity of the evolution equation for vortex sheet strength after a certain time interval, we obtained a nearly singular distribution of vortex sheet strength and finally the calculation broke.

Figure 8 shows the results for desingularized equations with $\delta^2 = 0.1$ and $A = 0.0476$ $\sigma = 0.0005$, $\alpha = 0$, The inclusion of the surface-tension effects allowed to increase the time interval when the iteration process for γ_t was converged. In Fig. 8a we can see the roll-up process of the interface. Figure 8b shows the time sequence of the curvature distribution and Fig. 8c shows the time sequence of vortex sheet strength. At the end of the calculation we can see the irregular variation of the curvature of the vortex sheet and a nearly singular distribution of vortex sheet strength. When we use the Boussinesq approximation in this case ($A = 0.0476$) (which means that we actually drop the nonlinear term in Eq. (3.5)), the roll-up process of the interface is continued.

Figure 9a shows the time sequence of the interface profile and Fig. 9b the time sequence of vortex sheet strength for the same parameter as in Fig. 8 but this time for the Boussinesq

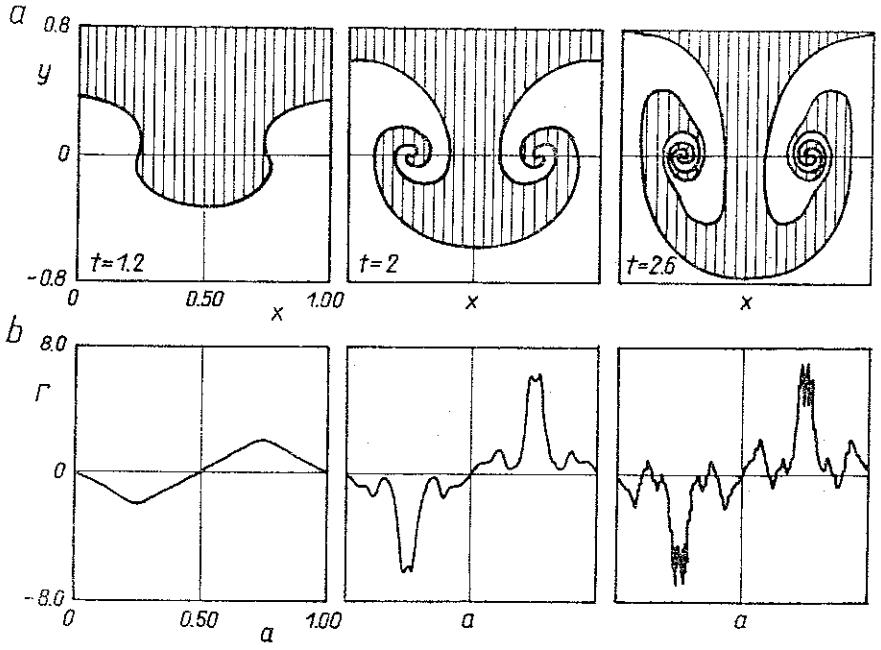

FIG. 9. Numerical results for desingularized equations, $\delta^2 = 0.1$, and for Boussinesq approximation $A = 0$. Surface tension is included $\sigma = 0.0005$, $N = 200$, $\alpha = 0$. Initial condition as in Fig. 2; a) time sequence of interface profiles b) time sequence of vortex sheet strength Γ vs Lagrangian parameter a. Values of t as shown in Fig. 9a.

approximation and $N = 200$. The amount of the roll-up depended on the size of δ^2. When δ^2 goes to zero, roll-up occurs earlier (see [13, 14, 11]).

In Fig. 10 we can see the difference in the shape of the interface for the different value of the Atwood number A for the same initial condition and in the same nondimensional time $t = 1.8$. The ability of interface roll-up decreases as the density ratio increases (one must take also into account the case $A = 1$ presented in Fig. 1a). The value of α parameter through Eq. (3.2) determines how the points are spread along the interface. KERR [11] stated that the best results can be obtained for $\alpha = -|A|^2$. It is a good initial estimation for α but experimentally one can determine a little different value for α as the best one. The wrong selection of α value makes the iteration process for γ_t stop very soon and from the oscillating curvature distribution one can see that all points have a different value of curvature.

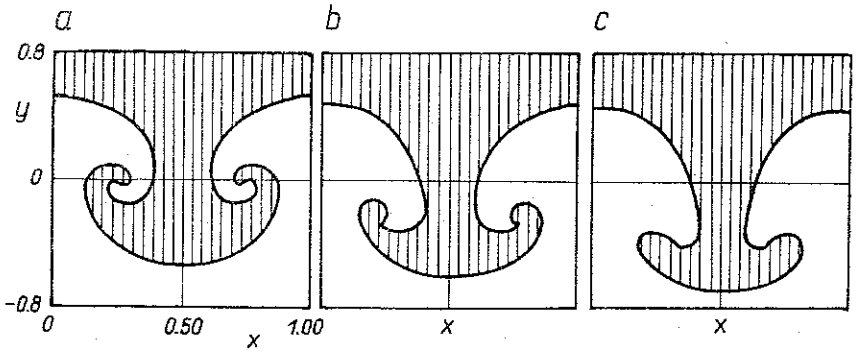

FIG. 10. Interface profile for various density ratios, and the same initial conditions $y(x, 0) = 0.1\cos 2\pi x$, $\gamma(x, 0) = 0$, $N = 120$, $\sigma = 0.0005$ and $\delta^2 = 0.1$. The nondimensional time is $t = 1.8$ in all cases; a) $A = 0.0476$ $(\varrho_1/\varrho_2 = 1.1)$, $\alpha = -0.05$, b) $A = 0.333\ldots$ $(\varrho_1/\varrho_2 = 2)$, $\alpha = -0.15$, c) $A = 0.5$ $(\varrho_1/\varrho_2 = 3)$, $\alpha = -0.2$.

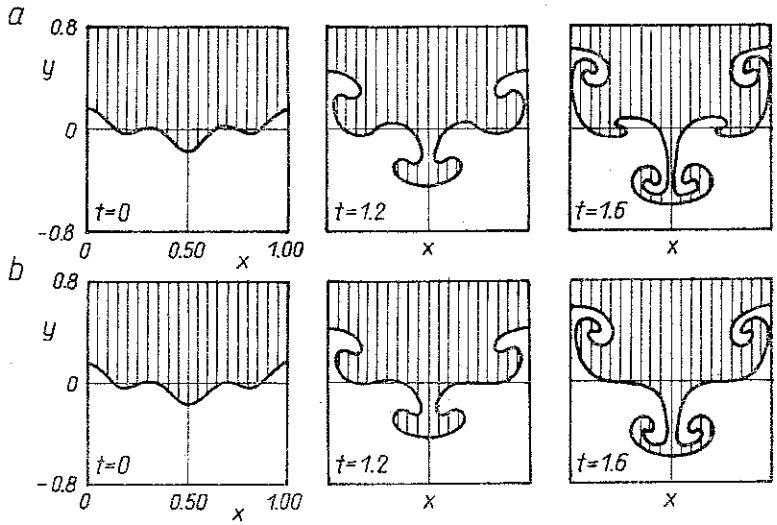

FIG. 11. Interface for $A = 0$, $\delta^2 = 0.1$, $\alpha = 0$, $N = 200$ and initial comndition $y(x, 0) = 0.1\cos 2\pi x + 0.07\cos 6\pi x$, $\gamma(x, 0) = 0$; a) $\sigma = 0$, no surface tension, b) $\sigma = 0.001$.

Figures 11a, b show the time sequence profile with and without surface tension effects for $A = 0$ (Boussinesq approximation), $\delta^2 = 0.1$, $\alpha = 0$, and for more complex two-wave initial perturbation as was described by AREF [1], viz. $y(x, 0) = \varepsilon_1 \cos 2\pi x + \varepsilon_2 \cos 6\pi x$, where ε_1, ε_2 were chosen in such a way that the initial profile had six inflection points. As it can be seen in Fig. 11a ($\sigma = 0$), six vortices grow from those six inflection points. But in Fig. 11b the surface-tension effect prevents the initiation of the vortex in the line $y = 0$. In this case we choose $N = 200$, and the coefficient for the interface surface tension σ is two times greater than in the previous run viz. $\sigma = 0.001$. This smoothing action of surface-tension effects is in good qualitative agreement with the results obtained by DALY in the numerical study of the R-T instability using the marker-in-cell method for full Navier–Stokes equations [8].

5. Conclusions

The inclusion to vortex sheet strength evolution equation surface-tension effects causes the suppression of irregular motion of vortices. The surface-tension effects provide a small scale stabilizing mechanism and don't remove ill-posedness of the problem. Singularity formations are the main reason for which the B-M-O method fails for $0 < A < 1$. Desingularization for the R-T problem by δ^2 is not so efficient as was demonstrated by KRASNY for vortex sheets in a constant density [13, 14]. Due to the nonlinearity of the evolution equation for the vortex sheet strength, after a certain time we obtained a nearly singular distribution of vortex sheet strength and finally the calculation broke. The lowering of the order of method for the solution of the differential equation and process of redistribution of the vortex along the interface as it was described by KERR [11] improves the situation only for a short time. As an alternative to the direct summation method, the vortex-in cell methods described by TRYGGVASON [23] are very computationally efficient. But as Tryggvason says the "grid free method although considerably more inefficient"... than the vortex in the cell method..." offers a "cleaner" environment (no grid disturbances) to study such delicate questions as singularity formations and how to apply proper regularizations".

References

1. H. AREF, *Finger bubble, tendril, spike*, Fluid Dynamics Trans., **13**, pp. 25–54, PWN, Warsaw 1987.
2. G. R. BAKER, D. I. MEIRON and S. A. ORSZAG, *Vortex simulation of the Rayleigh–Taylor instability*, Phys. Fluids, **23**, pp. 1485–1490, 1980.
3. G. R. BAKER, D. I. MEIRON and S. A. ORSZAG, *Generalized vortex methods for free surface flow problems*, J. Fluid Mech., **123**, pp. 477–501, 1982.
4. G. R. BAKER, *Generalized vortex methods for free-surface flows*, Proc Wave on Fluid Interface, pp. 53–81, Academic Press 1983.
5. R BELLMAN and R. H. PENNINGTON, *Effects of surface tension and viscosity on Taylor instability*, Quart. Appl. Math., **12**, pp. 151–162, 1954.
6. G. BIRKHOFF, *Helmholtz and Taylor instability*, Proc. Symp. Appl. Math., Am. Math. Soc, R. I., Providence 1962.
7. A. J. CHORIN and P. S. BERNARD, *Discretization of a vortex sheet with an example of roll-up*, J. Comp. Phys., **13**, pp. 423–429, 1973.
8. B. J. DALY, *Numerical study of the effect of surface tension on interface instability*, Phys. Fluids, **12** pp. 1340–1354, 1969.

9. P. T. FINK and W. K. SOH, *A new approach to roll-up calculations of vortex sheets*, Proc. Roy. Soc., Serie A, **362**, pp. 195–209, 1978.
10. F. G. GAHOV, *Boundary problems*, Mir, Moscow 1977 (in Russian).
11. R. M. KERR, *Simulation of Rayleigh–Taylor flows using vortex blobs*, J. Comp. Phys., **76**, pp. 48–84, 1988.
12. R. KRASNY, *A study of singularity formation in a vortex sheet by the point-vortex approximation*, J. Fluid Mech., **167**, p . 65–93, 1986.
13. R. KRASNY, *Desingularization of periodic vortex sheet roll-up*, J. Comp. Phys., **65**, pp. 292–313, 1986.
14. R. KRASNY, *Computation of vortex sheet roll-up in the Treffitz plane*, J. Fluid Mech., **184**, pp. 123–155, 1987.
15. H. KUDELA, *A study on the generalized vortex method for Rayleigh–Taylor instability*, Intern. Seminar on Engineering Applications of the Surface and Cloud Vorticity Methods, Part II, 1986; Scientific Papers of the Institute of Machine Construction and Operation of Technical University of Wrocław 51, pp. 53–62, 1987.
16. D. I. MEIRON, G. R. BAKER and S. A. ORSZAG, *Analytic structure of vortex sheet dynamics. Part I. Kelvin–Helmholtz instability*, J. Fluid Mech., 114, pp. 83–298, 1982.
17. M. S. LONGUET-HIGGINS and E. L. COKELET, *The deformation of steep surface waves on water. I. A numerical method of computation*, Proc. Roy. Soc., Serie A, **350**, pp. 1–26, 1976.
18. R. MENIKOFF and C. ZEMACH, *Rayleigh–Taylor instability and the use of conformal maps for ideal fluid flow*, J. Comp. Phys., **51**, pp. 28–64, 1983.
19. D. W. MOORE, *On the point vortex method*, SIAM J. Sci. Stat. Computat., **2**, pp. 65–84, 1981.
20. D. W. MOORE, *Numerical and analytical aspects of Helmholtz instability*, Theoretical and Applied Mechanics, IUTAM, pp. 263–274, 1985.
21. D. I. PULLIN, *Numerical studies of surface-tension effects in nonlinear Kelvin–Helmholtz and Rayleight–Taylor instability*, **119**, pp. 507–532, 1982
22. D. H. SHARP, *An overview of Rayleigh–Taylor instability*, Physica, **12D**, pp. 3–18, 1984.
23. G. TRYGGVASON, *Numerical simulation of the Rayleigh–Taylor instability*, J. Comp. Phys., **75**, pp. 253–282, 1988.

TECHNICAL UNIVERSITY OF WROCŁAW, WROCŁAW.

Received November 17, 1989.